

# Performance of Drought Indices on Maize Production in Northern Nigeria Using Artificial Neural Network Model

Adedayo A. Adepoju<sup>a,1,\*</sup>, Tayo P. Ogundunmade<sup>a,2</sup>, Grace O. Adenuga<sup>a,3</sup>

<sup>a</sup> Department of Statistics, University of Ibadan, Ibadan, Nigeria

<sup>1</sup> [pojuday@yahoo.com](mailto:pojuday@yahoo.com); <sup>2</sup> [ogundunmadetayo@yahoo.com](mailto:ogundunmadetayo@yahoo.com); <sup>3</sup> [olamy97@gmail.com](mailto:olamy97@gmail.com)

\* corresponding author

## ARTICLE INFO

### Article history

Received March 15, 2023

Revised December 17, 2023

Accepted January 10, 2024

### Keywords

artificial neural network

drought indices

mean square error

activation functions

maize yield

## ABSTRACT

Drought is widely known to put the ecosystem at risk. It ensues when there is a major rainfall shortage that causes hydrological discrepancies and alters the land productive structures. The degree of rainfall influences the growth and harvests of maize, particularly where irrigation is not practicable. In some parts of northern Nigeria, rainfall is unpredictable and often lower than the quantity needed for a viable crop. For the detection, classification, and control of drought conditions, drought indices are used. There has been notable progress in the last few years in terms of modelling droughts by utilizing statistical or physical models. Despite the successes documented by most of these approaches; a plain, effective, and well-built statistical model is the artificial neural network (ANN). The use of artificial neural networks (ANN) to evaluate the impact of drought indices on maize output in the 17 northern Nigerian states is presented in this research. For a 25-year period from 1993 to 2018, observed annual data of drought indices, RDI, and the Palmer drought indices, which comprise SCPDSI, SCPHDI, and SCWLPM, as well as maize yield (measured in tonnes) in Northern states of Nigeria. The ANN model was evaluated using several activation functions (sigmoid, hyperbolic tangent, and rectified linear unit), hidden layers (1, 2, and 3), and training sets (70%, 80%, and 90%). The Mean Square Error (MSE) was employed to evaluate each ANN model's performance. In summary, most of the states' lowest mean square errors (MSEs) were generated via RELU. Also, as the training percentage increases, the mean square error increases.

This is an open access article under the [CC-BY-SA](https://creativecommons.org/licenses/by-sa/4.0/) license.



## 1. Introduction

The natural world is widely known to be at risk during droughts. It results from significant rainfall deficits that modify the land's productive structures and create hydrological disparities. According to Um et al. (2017), droughts occur in all climatic regions, regardless of monthly rainfall averages. Drought is thought to be an ecological disaster distinct from other environmental disasters due to its stable character (Yue et al. 2018). Liu et al. (2018) discussed how droughts develop gradually and have long-lasting effects that spread slowly and become critical over time, even after they have ended. According to research, droughts, often referred to as dry spells at the beginning or end of each season, have been occurring continuously since the turn of the 20th century (Lester, 2006). This is a common occurrence in the Sudano-Sahelian region of Nigeria, yet there has recently been a significant amount of ambiguity around it. It has the potential to wipe out humanity, the physical biosphere, and agricultural products (Gidey et al., 2018). This is accurate given that large portions of Northern Nigeria are situated between 9 and 14 degrees north latitude, inside the Sahel and Sudan regions, which are frequently affected by droughts (Nyong et al., 2007). The six vegetation zones that

make up Nigeria are the Sahel grassland vegetation areas, the Coastal Mangrove Swamp Forest, the Rainforest, Southern Guinea, Northern Guinea, and Sudan. Local variations exist between these vegetations in terms of weather structure. One of the most important food crops in Nigeria is maize, a cereal of great importance. Owing to its inherent adaptability, it is the most extensively cultivated crop in the nation, growing in both the arid Sudan savanna and the moist evergreen forest zone. Its insensitivity to photoperiod allows it to be cultivated year-round, giving it even more versatility non terms of growth methods. In the Guinea and Sudan savannas of northern Nigeria, it is one of the most significant grain crops. Traditional crops like sorghum and millet have lately lost ground to maize as a major crop. With 10.2 million tons of maize harvested from 4.8 million hectares in 2018, Nigeria emerged as Africa's top producer (FAO, 2018). Agronomists and breeders have worked together to develop several technologies, including as low-nitrogen, disease-resistant, drought-resistant, and Striga-resistant cultivars. (Kamara and others, 2014). Harvests in the Nigerian savannas remain low despite the availability of these types.

There are numerous records of drought events that caused famines in Northern Nigeria, including the droughts of 1903 and 1911–1914 (Shiru et al., 2018). According to Abaje et al. (2013), there were more droughts in 1919, 1924, 1935, 1951 to 1954, 1972 to 1973, 1984 to 1985, 2007, and 2011. Farming is the most profitable industry in the area. In addition, the area is well-known for its agricultural products, which include wheat, sorghum, millet, and maize (Eze, 2017). Nigerian agriculture, especially in the north, depends primarily on rain and is thus subject to the vagaries of unpredictable rainfall patterns (Tihamiyu et al., 2015). Due to the years of heavy rainfall, households in the area have enjoyed bountiful harvests from both agricultural and animal husbandry. Conversely, in the event of insufficient rainfall, the household experiences low crop productivity and crop failure, resulting in animal deaths and malnutrition. (Eze and colleagues, 2018).

Drought indices are used to identify, categorize, and regulate drought situations. They support decision-making processes by enabling the quantitative assessment of the degree, duration, and spatial scope of aberrant weather circumstances. The Standardized Precipitation Index (SPI), Standardized Precipitation Evapotranspiration Index (SPEI), Palmer Drought Severity Index (PDSI), Standardized Runoff Index (SRI), and Reconnaissance Drought Index (RDI) are just a few of the many drought indices that have been developed to evaluate droughts. SPI and PDSI are the two most often utilized indices among them (Tsakiris et al., 2005). People in this region of the country are greatly distressed by the drought crisis, but politicians are either unaware of the causes of the issue or have not given them much thought. The degree to which the most widely used drought indices can determine the effects of drought on susceptible systems is now the subject of a scant systematic investigation. This study's primary goal is to evaluate the impact of drought indicators on maize output in Nigeria's northern region by utilizing artificial neural networks (ANNs). The remainder of the piece is organized as follows: The findings and discussion are presented in section three, the material and methodology are presented in section four, and the conclusion is given in section five.

## 2. Materials and Methods

### 2.1 Study Area and Data

Nigeria, a country in West Africa is the largest country in Africa. It has distinguished demographic characteristics in Sub-Saharan Africa and shares a border in the North with Niger, at North East Chad, at East Cameroon and also Benin in the west region. Nigeria at 9.0820° N, 8.6753 ° E is a tropical region at the extreme inner corner Gulf of guinea which is on the west coast of Africa, which has an area of 923,768 square km and a coastline of 85km. the country is 1,045 km long and 1,126 km wide. Nigeria comprises 36 states and the country capital Abuja which has the Federal Capital Territory. Nigeria is made up of 36 states plus the Federal Capital Territory, which is located in Abuja, the nation's capital. There are six geopolitical zones in Nigeria. Nigeria's states and geopolitical zones are home to a diverse range of ethnic groups and cultures. Although there are many more religions practiced in the nation, Islam and Christianity are the two most common. Historically, Islam has shaped the culture of the northern part of the nation, which is home to several

significant Islamic states. In the past, the southern areas were home to mighty states like the Ife Confederacy, the Oyo Empire, and the Benin Empire. Nigeria's culture was greatly impacted by British colonial authority, which introduced English as the primary official language rather than any of the more than 500 regional languages spoken there.

Desertification is being brought on by decreasing rainfall in Northern Nigeria's already-deserted areas. The Sahara Desert is moving southward at a rate of 0.6 km annually, yet the northern region of Nigeria is blessed with a vast area of arable land that has historically provided a key means for farming and other economic operations (Abubakar, 2013). Because of this, Nigeria loses over 350,000 hectares of land to desertification each year. Communities in 11 states in the North have seen a change in population as a result of this. It is estimated that Nigeria loses over \$5 billion annually due to drought and rapid desertification. Desertification is putting over 5 million farm animals at risk of extinction.

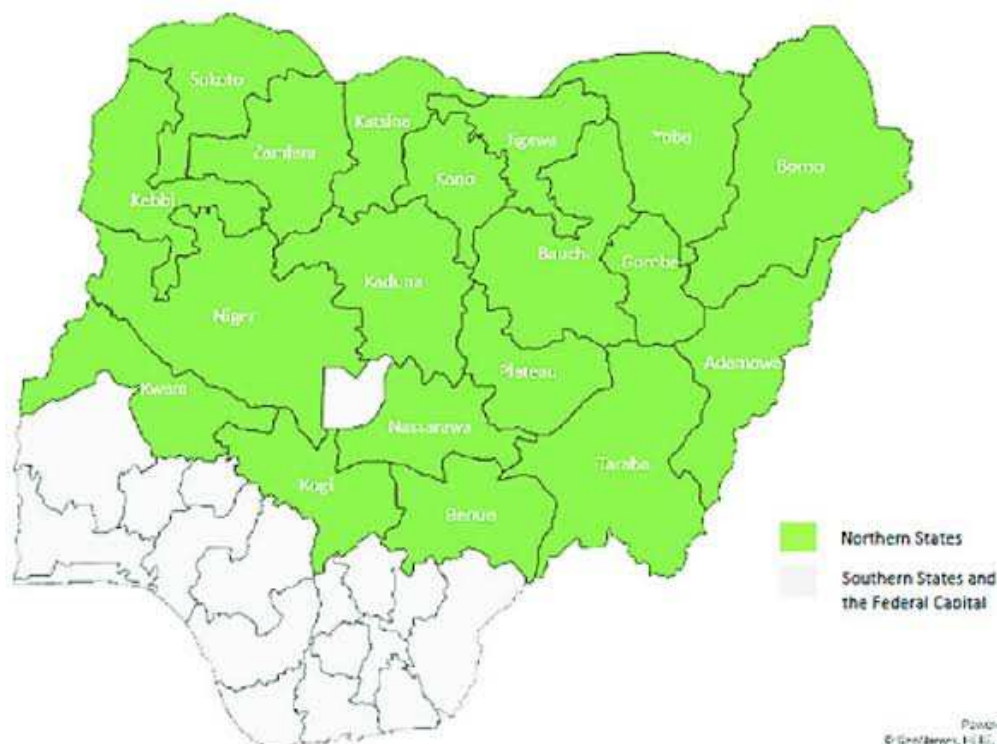


**Figure 1.** Map of Nigeria showing the Northern states, Saki et al., (2019)

The 19 states that make up the Northern region of Nigeria are divided into the North East, North West, and North Central geopolitical zones, along with the Federal Capital Territory. The states of Adamawa, Bauchi, Borno, Gombe, Taraba, and Yobe are included in the Northeast region. The states of Jigawa, Kaduna, Kano, Katsina, Kebbi, Sokoto, and Zamfara are included in the North West. The states of Benue, Kogi, Kwara, Nasarawa, Niger, Plateau, and FCT are all part of North Central. The seventeen (17) Northern Nigerian states of Adamawa, Bauchi, Borno, Gombe, Yobe, Kano, Katsina, Kebbi, Sokoto, and Zamfara, as well as the states of Benue, Kogi, Kwara, Nasarawa, Niger, Plateau, and Federal Capital Territory, were the subjects of this study. The Palmer drought indices, which comprise SCPDSI, SCPHDI, and SCWLPM, as well as observed annual data on drought indices and maize yield (measured in tonnes) in Northern states of Nigeria were acquired. The collected information spanned 25 years, from 1993 to 2018.

SCPDSI stands for Self-calibrated Palmer drought severity index

SCPHDI stands for Self-calibrated Palmer hydrological drought index

SCWLPM stands for Modified/Weighted Palmer drought severity index

RDI stands for Reconnaissance Drought Index.

## 2.2 Artificial Neural Network (ANN)

ANNs are straightforward statistical models that have been applied to a wide range of tasks in the engineering, earth science, medical, hydrological, and other fields. These tasks include forecasting, curve-fitting, and regression. ANN models analyze data and perform tasks like predicting and classification. Unlike other models that rely on prior postulations, the network model in the building procedure is evaluated based on the nature of the data. The levels of an ANN arrangement are arranged as input, hidden, and output levels. Every level has neurons, which are linked components. The key components of the ANN models used to fix a hitch are their weights. To prevent the output from growing larger, the weighted input total as well as the bias terms are fed into an activation function. Sets of activation functions that are often used are the Rectified Linear unit (ReLU), hyperbolic tangent, and sigmoid functions.

$$y = f(x) + ei = \sum x_i w_i + ei \quad (1)$$

$$\text{Output} = \text{sum}(\text{weights} * \text{inputs}) + \text{bias} \quad (2)$$

Inputs: RDI , SCPDSI, SCPHDI and SCWLPM

Output: maize yield in tonnes

In conclusion, the information supplied to the input layer introduces the dissemination of facts. As a result, the network modifies its weights and applies a learning algorithm to choose a combination of weights that produces the least amount of error. We call this process "training." A current independent testing set is utilized to validate the trained model following the completion of the training process. An effective way to stop overfitting and simplify is to use a dropout regularization technique.

### 2.2.1 ANN Model Development

To estimate the drought indices and maize yield in this study, a multilayer perceptron (MLP) feed-forward network was employed. By updating the weights between each node, the multilayer perceptron decreased the error between the observed values and the outputs of the ANN model. Important issues arise from the extremely nonlinear nature of the observed variables and their multiple interrelations in the modeling of hydrological processes. The amount of hidden neurons and nodes, together with the selection of an appropriate model architecture, are critical factors in modeling such large inputs. As of now, there are no exact approaches for issues like the number of hidden layers and hidden nodes that ought to be included in an ANN model. To determine the ideal number of nodes for the hidden layer, a trial-and-error approach was therefore adopted. For this study, the data was divided into training and test sets. The test data were not included in the process of creating the artificial neural network (ANN) model, which was used to assess the predictive power of the model over the 25-year period from 1993 to 2018. The test data were divided into different training and testing sets (70%, 80%, 90%), hidden layers (1, 2, 3), and activation functions (sigmoid, hyperbolic tangent, repaired linear unit). As a result, the findings in the results section represent estimates of the ANN's performance using the test set of data. The following equations are used to normalize all of the input data.

$$Y_i = \frac{X_{oi}}{X_{o\max}}, X_{oi} \geq 0 \quad (3)$$

$$Y_i = \frac{X_{oi}}{|X_{o\min}|}, X_{oi} < 0 \quad (4)$$

Where  $X_{oi}$  is the observed value,  $X_{o\min}$  and  $X_{o\max}$  are respectively the minimum and maximum data in the input time series.

### 2.2.2 Activation functions

The basic way to perceive how neural networks are handled is by using their activation functions. A mathematical function that converts an input variable to an output variable is called an activation function. Neural networks operate similarly to linear functions by default for activation functions. When the input and output variables are exactly related, the function is said to be linear.

However, the majority of the constraints that neural networks attempt to solve are intricate and nonlinear. To achieve the nonlinearity, the activation functions are employed. High-level polynomial functions are known as nonlinear functions. A nonlinear function's graph combines the complicating factor and is curved. Activation functions provide neural networks their nonlinearity and make them precise approximations of universal functions.

#### A. Sigmoid

The sigmoid function is a mathematical function that gives a sigmoidal curve; a characteristic curve for its S shape. This is the oldest and frequently used activation function. This compresses the input to any value between 0 and 1 and makes the model logistic. This function is known as a special case of logistic function defined by the following formula:

$$f(x) = 1/(1 + e^{-x}) \quad (5)$$

#### B. Hyperbolic tangent

Another common and mostly utilized activation function is the tanh function. This is a nonlinear function, characterized in the scale of values (-1, 1). One thing to make clear is that the gradient is better for tanh than sigmoid (the derivatives are steeper). Settling between sigmoid and tanh will be based on the gradient strength prerequisite. Like the sigmoid, tanh also has the missing slope constraint. The function is specified by the formula:

$$f(x) = \tanh(x) \quad (6)$$

This looks like sigmoid; it is a scaled sigmoid function.

#### C. Rectified Linear Unit

Rectified Linear Unit (ReLU) is a predominantly utilized activation function. It is a simple specification and has merits over the other functions. The function is defined by the following formula:

$$f(x) = 0 \text{ when } x < 0 \\ x \text{ when } x \geq 0 \quad (3)$$

The scale of the result is between 0 and infinity. RELU finds usage in computer vision and speech identification using deep neural networks.

### 2.3 Model Performance Measures

In this study, to assess the performances of all ANN models, the goodness of fit measure namely Mean Square Error (MSE) is utilized.

$$\text{Mean Absolute Percentage Error} = \left[ \frac{1}{n} \sum_{i=1}^n (X_{oi} - X_{ci})^2 \right] \quad (3)$$

Where  $X_{oi}$  = observed value,  $X_{ci}$  = predicted value

MSE is used to calculate the mean ANN model prediction error to reveal how close the predicted values are to the observed. Lesser values of the index imply optimum prediction precision.



### 3. Analysis, Results and Discussion

The information provided here is based on an examination of data from the Nigeria Metrological Agency (NIMET) regarding maize yield and drought indices. Maize yield, RDI, SCPDSI, SCWLPM, and SCPHDI are the variables taken into account.

**Table 1.** ANN Results for North Central states

NORTH CENTRAL									
Activation functions	Training: 70%; Testing: 30%			Training:80%; Testing:20%			Training:90%; Testing:10%		
	Hidden layer (1)	Hidden layer (2)	Hidden layer (3)	Hidden layer (1)	Hidden layer (2)	Hidden layer (3)	Hidden layer (1)	Hidden layer (2)	Hidden layer (3)
RELU	<b>0.8618</b>	1.0411	1.0411	<b>1.1034</b>	1.2462	1.2388	<b>1.6480</b>	<b>1.6480</b>	1.6497
Sigmoid	1.1255	<b>0.8225</b>	1.1397	1.1182	<b>1.0731</b>	1.1873	1.8472	<b>1.6085</b>	1.7458
Hyperbolic tangent	1.1736	<b>1.1296</b>	1.1704	<b>1.1068</b>	1.1199	1.1488	1.7873	1.9465	<b>1.6685</b>
Activation functions	Training: 70%; Testing: 30%			Training:80%; Testing:20%			Training:90%; Testing:10%		
	Hidden layer (1)	Hidden layer (2)	Hidden layer (3)	Hidden layer (1)	Hidden layer (2)	Hidden layer (3)	Hidden layer (1)	Hidden layer (2)	Hidden layer (3)
RELU	<b>0.2093</b>	0.3887	0.4031	<b>0.2943</b>	0.2984	0.2958	0.4151	<b>0.4145</b>	0.4146
Sigmoid	<b>0.3292</b>	0.4244	0.4171	0.4832	<b>0.2680</b>	0.4132	0.5302	<b>0.4836</b>	0.5583
Hyperbolic tangent	0.3427	0.3301	<b>0.3127</b>	0.4610	<b>0.2640</b>	0.7495	<b>0.4691</b>	0.6112	0.8081
Activation functions	Training: 70%; Testing: 30%			Training:80%; Testing:20%			Training:90%; Testing:10%		
	Hidden layer (1)	Hidden layer (2)	Hidden layer (3)	Hidden layer (1)	Hidden layer (2)	Hidden layer (3)	Hidden layer (1)	Hidden layer (2)	Hidden layer (3)
RELU	0.0865	<b>0.0443</b>	0.3492	0.1092	<b>0.0415</b>	<b>0.0415</b>	0.1723	0.1725	<b>0.1705</b>
Sigmoid	<b>0.0879</b>	0.1034	0.0965	0.0739	0.0984	<b>0.0444</b>	<b>0.0835</b>	0.1009	0.0923
Hyperbolic tangent	0.0874	0.0442	<b>0.0420</b>	0.1141	0.1085	<b>0.0509</b>	<b>0.0816</b>	0.1067	0.1832
Activation functions	Training: 70%; Testing: 30%			Training:80%; Testing:20%			Training:90%; Testing:10%		
	Hidden layer (1)	Hidden layer (2)	Hidden layer (3)	Hidden layer (1)	Hidden layer (2)	Hidden layer (3)	Hidden layer (1)	Hidden layer (2)	Hidden layer (3)
RELU	0.0865	<b>0.0443</b>	0.3492	0.1092	<b>0.0415</b>	<b>0.0415</b>	0.1723	0.1725	<b>0.1705</b>
Sigmoid	<b>0.0879</b>	0.1034	0.0965	0.0739	0.0984	<b>0.0444</b>	<b>0.0835</b>	0.1009	0.0923
Hyperbolic tangent	0.0874	0.0442	<b>0.0420</b>	0.1141	0.1085	<b>0.0509</b>	<b>0.0816</b>	0.1067	0.1832

	Hidden layer (1)	Hidden layer (2)	Hidden layer (3)	Hidden layer (1)	Hidden layer (2)	Hidden layer (3)	Hidden layer (1)	Hidden layer (2)	Hidden layer (3)
RELU	<b>0.5379</b>	0.5455	0.5412	0.7403	<b>0.7392</b>	0.7511	<b>1.1789</b>	<b>1.1789</b>	1.3083
Sigmoid	0.5236	0.5344	<b>0.5229</b>	0.7373	0.7372	<b>0.6853</b>	1.1200	1.1571	<b>1.0512</b>
Hyperbolic tangent	0.5451	0.4877	<b>0.4577</b>	0.7251	0.7370	<b>0.6132</b>	<b>1.0845</b>	1.1386	0.9467
Activation functions	Training: 70%; Testing: 30%			Training:80%; Testing:20%			Training:90%; Testing:10%		
	Hidden layer (1)	Hidden layer (2)	Hidden layer (3)	Hidden layer (1)	Hidden layer (2)	Hidden layer (3)	Hidden layer (1)	Hidden layer (2)	Hidden layer (3)
RELU	0.1072	0.0571	<b>0.0509</b>	0.1103	0.0786	<b>0.0779</b>	<b>0.1252</b>	0.1253	<b>0.1252</b>
Sigmoid	0.0694	<b>0.0553</b>	0.0582	0.0811	<b>0.0730</b>	0.0869	0.1044	<b>0.0933</b>	0.2655
Hyperbolic tangent	0.0891	<b>0.0456</b>	0.1433	0.0887	0.1217	<b>0.0659</b>	0.0938	0.0982	<b>0.0346</b>
Activation functions	Training: 70%; Testing: 30%			Training:80%; Testing:20%			Training:90%; Testing:10%		
	Hidden layer (1)	Hidden layer (2)	Hidden layer (3)	Hidden layer (1)	Hidden layer (2)	Hidden layer (3)	Hidden layer (1)	Hidden layer (2)	Hidden layer (3)
RELU	<b>0.5677</b>	0.7898	0.7187	<b>0.7316</b>	1.0803	1.0940	0.5145	<b>0.5144</b>	0.5145
Sigmoid	<b>0.8247</b>	1.4967	3.1551	1.2070	<b>0.7519</b>	1.8062	<b>0.5309</b>	0.5395	0.7106
Hyperbolic tangent	<b>0.9518</b>	2.4355	2.2076	0.7352	<b>0.7314</b>	1.2816	0.5528	<b>0.5442</b>	1.6639
Activation functions	Training: 70%; Testing: 30%			Training:80%; Testing:20%			Training:90%; Testing:10%		
	Hidden layer (1)	Hidden layer (2)	Hidden layer (3)	Hidden layer (1)	Hidden layer (2)	Hidden layer (3)	Hidden layer (1)	Hidden layer (2)	Hidden layer (3)
RELU	<b>1.7512</b>	2.3996	2.1158	<b>1.4044</b>	1.6851	1.6611	2.3157	<b>1.6391</b>	2.3156
Sigmoid	<b>2.0473</b>	2.2249	2.1263	<b>1.4017</b>	1.4581	6.1841	<b>2.4169</b>	5.4464	6.9884
Hyperbolic tangent	<b>2.0807</b>	2.4621	2.7287	5.6880	<b>1.3101</b>	6.8431	<b>2.3414</b>	6.2315	21.6894

The minimum MSE values in Nassarawa state are as follows: Sigmoid (0.8225) at 70% training set, Sigmoid (1.0731) at 80% training set, and Sigmoid (1.6085) at 90% training set. Thus, with 90% training set, sigmoid has the lowest MSE value. The minimal MSE values for Kogi state are as follows: RELU (0.2093) at 70% training set, Hyperbolic tangent (0.2640) at 80% training set, and RELU (0.4145) at 90% training set. Consequently, with a 70% training set, RELU has the lowest MSE value. The minimum MSE value for Kwara state is found at 70% training set for Hyperbolic tangent (0.0420), 80% training set for RELU (0.0415), and 90% training set for Hyperbolic tangent (0.0816). With an 80% training set, RELU therefore has the lowest MSE value. In the state of Niger, the least mean square error (MSE) is found for Hyperbolic tangent (0.4577) at 70%, Hyperbolic tangent (0.6132) at 80%, and Hyperbolic tangent (0.9467) at 90% of training sets. As a result, at 70% training set, the hyperbolic tangent has the lowest MSE value. In the Plateau state, the minimal mean square error (MSE) is found for Hyperbolic tangent (0.0456) at 70%, Hyperbolic tangent (0.0659) at 80%, and Hyperbolic tangent (0.0346) at 90% of the training sets. As a result, at 90% training set, the hyperbolic tangent has the lowest MSE value. The minimum MSE value in FCT is found at 70% training set for RELU (0.5677), 80% training set for Hyperbolic tangent (0.7314), and 90% training set for RELU (0.5144). Hence, at 90% training set, ReLU has the lowest MSE value. As a result, at 70% training set, the hyperbolic tangent has the lowest MSE value. In the Plateau state, the minimal mean square error (MSE) is found for Hyperbolic tangent (0.0456) at 70%, Hyperbolic tangent (0.0659) at 80%, and Hyperbolic tangent (0.0346) at 90% of the training sets. As a result, at 90% training set, the hyperbolic tangent has the lowest MSE value. The minimum MSE value in FCT is found at 70% training set for ReLU (0.5677), 80% training set for Hyperbolic tangent (0.7314), and 90% training set for ReLU (0.5144). Hence, at 90% training set, ReLU has the lowest MSE value.

**Table 2.** ANN Results for North East states

NORTH EAST										
ADAMAWA STATE	Activation functions	Training: 70%; Testing: 30%			Training:80%; Testing:20%			Training:90%; Testing:10%		
		Hidden layer (1)	Hidden layer (2)	Hidden layer (3)	Hidden layer (1)	Hidden layer (2)	Hidden layer (3)	Hidden layer (1)	Hidden layer (2)	Hidden layer (3)
RELU		0.370	0.398	<b>0.347</b>	<b>0.317</b>	0.317	0.320	0.476	0.518	<b>0.475</b>
		2	7	<b>9</b>	<b>2</b>	3	6	1	1	<b>6</b>
Sigmoid		<b>0.360</b>	0.906	0.822	0.292	0.302	<b>0.257</b>	0.463	<b>0.448</b>	0.475
		<b>2</b>	4	1	8	8	<b>1</b>	6	<b>5</b>	1
Hyperbolic tangent		<b>0.539</b>	0.709	1.719	<b>0.290</b>	0.317	0.388	0.449	<b>0.390</b>	<b>0.390</b>
		<b>1</b>	8	0	<b>3</b>	0	8	2	<b>6</b>	<b>6</b>
BAUCHI STATE										
		Training: 70%; Testing: 30%			Training:80%; Testing:20%			Training:90%; Testing:10%		



	Activation functions	Hidden layer (1)	Hidden layer (2)	Hidden layer (3)	Hidden layer (1)	Hidden layer (2)	Hidden layer (3)	Hidden layer (1)	Hidden layer (2)	Hidden layer (3)
RELU	1.389	1.063	<b>1.026</b>	0.271	0.235	<b>0.207</b>	<b>0.100</b>	0.100	0.106	
	4	9	<b>3</b>	8	8	<b>4</b>	<b>6</b>	7	4	
Sigmoid	1.149	1.101	<b>1.093</b>	0.208	<b>0.175</b>	0.269	0.269	<b>0.151</b>	0.202	
	0	1	<b>7</b>	2	<b>6</b>	6	5	<b>3</b>	0	
Hyperbolic tangent	1.296	1.127	<b>1.124</b>	0.523	<b>0.243</b>	0.519	0.220	0.312	<b>0.015</b>	
	5	1	<b>5</b>	4	<b>9</b>	7	7	6	<b>9</b>	

BORNO STATE	Activation functions	Training: 70%; Testing: 30%			Training: 80%; Testing: 20%			Training: 90%; Testing: 10%		
		Hidden layer (1)	Hidden layer (2)	Hidden layer (3)	Hidden layer (1)	Hidden layer (2)	Hidden layer (3)	Hidden layer (1)	Hidden layer (2)	Hidden layer (3)
RELU	<b>0.073</b>	0.218	0.125	<b>0.094</b>	0.118	0.119	0.064	0.064	<b>0.058</b>	
	<b>2</b>	3	2	<b>5</b>	0	3	4	3	<b>9</b>	
Sigmoid	<b>0.106</b>	0.115	0.123	<b>0.075</b>	0.127	0.100	0.078	0.075	<b>0.061</b>	
	<b>4</b>	9	2	<b>1</b>	4	0	4	7	<b>0</b>	
Hyperbolic tangent	<b>0.134</b>	0.150	0.142	0.110	<b>0.087</b>	0.128	0.117	<b>0.080</b>	0.357	
	<b>9</b>	5	2	7	<b>7</b>	7	3	<b>6</b>	1	

GOMBE STATE	Activation functions	Training: 70%; Testing: 30%			Training: 80%; Testing: 20%			Training: 90%; Testing: 10%		
		Hidden layer (1)	Hidden layer (2)	Hidden layer (3)	Hidden layer (1)	Hidden layer (2)	Hidden layer (3)	Hidden layer (1)	Hidden layer (2)	Hidden layer (3)
RELU	0.171	0.256	<b>0.157</b>	<b>0.108</b>	0.182	0.177	0.180	<b>0.156</b>	0.178	
	2	7	<b>5</b>	<b>1</b>	8	8	9	<b>3</b>	1	
Sigmoid	<b>0.134</b>	0.185	0.173	0.210	0.192	<b>0.187</b>	0.300	<b>0.288</b>	0.334	
	<b>8</b>	3	5	7	9	<b>1</b>	0	<b>1</b>	4	
Hyperbolic tangent	<b>0.132</b>	0.160	0.218	0.202	<b>0.111</b>	0.203	0.295	0.307	<b>0.239</b>	
	<b>2</b>	8	7	7	<b>6</b>	4	8	9	<b>3</b>	

YOBE STATE	Activation functions	Training: 70%; Testing: 30%			Training:80%; Testing:20%			Training:90%; Testing:10%		
		Hidden layer (1)	Hidden layer (2)	Hidden layer (3)	Hidden layer (1)	Hidden layer (2)	Hidden layer (3)	Hidden layer (1)	Hidden layer (2)	Hidden layer (3)
RELU		<b>0.436</b> 2	0.472 7	0.695 0	<b>0.315</b> 5	0.601 7	0.616 8	0.451 2	0.963 8	<b>0.450</b> 9
Sigmoid		0.511 8	0.526 3	<b>0.387</b> 1	0.746 8	0.636 8	<b>0.442</b> 8	1.084 4	0.982 6	<b>0.835</b> 3
Hyperbolic tangent		0.505 1	0.711 0	<b>0.492</b> 5	0.789 7	<b>0.364</b> 3	0.718 8	1.216 8	<b>1.006</b> 5	1.504 6

The lowest MSE values in Adamawa state are found at 70% training sets for RELU (0.3479), 80% training sets for Sigmoid (0.2571), and 90% training sets for Hyperbolic tangent (0.3906). Consequently, at 80% of the training set, sigmoid has the lowest MSE value. The minimal MSE values in Bauchi state are as follows: at 70% training set, RELU (1.0263), at 80% training set, Sigmoid (0.1756), and at 90% training set, Hyperbolic tangent (0.0159). As a result, at 90% training set, the hyperbolic tangent has the lowest MSE value. The lowest MSE values in Borno state are as follows: RELU (0.0732) at 70% training set, Sigmoid (0.0751) at 80% training set, and RELU (0.0589) at 90% training set. Hence, at 90% training set, RELU has the lowest MSE value. The minimal MSE values in Gombe state are found for the hyperbolic tangent (0.1322) at 70% training set, RELU (0.1081) at 80% training set, and RELU (0.1563) at 90% training set. Consequently, in the 80% training set, RELU has the lowest MSE value. The minimal mean square error (MSE) values in Yobe state are as follows: Sigmoid (0.3871), RELU (0.3155), and RELU (0.4509) at 70%, 80%, and 90% of the training sets, respectively. Consequently, in the 80% training set, RELU has the lowest MSE value. In conclusion, RELU fared better in the Northeast than the other activation functions. In Borno, Gombe, and Yobe states, correspondingly, it has the lowest MSE.

**Table 3.** ANN Results for North Western states  
**NORTH WEST**

KATSINA STATE	Activation functions	Training: 70%; Testing: 30%			Training:80%; Testing:20%			Training:90%; Testing:10%		
		Hidden layer (1)	Hidden layer (2)	Hidden layer (3)	Hidden layer (1)	Hidden layer (2)	Hidden layer (3)	Hidden layer (1)	Hidden layer (2)	Hidden layer (3)
RELU		<b>0.099</b> 3	0.135 9	0.133 6	<b>0.125</b> 1	0.144 7	0.145 4	0.476 1	0.5181	<b>0.475</b> 6

	Sigmoid	<b>0.102</b>	0.114	0.150	0.292	0.302	<b>0.257</b>	0.463	<b>0.4485</b>	0.475
		<b>5</b>	7	0	8	8	<b>1</b>	6		1
	Hyperbolic tangent	<b>0.150</b>	<b>0.150</b>	<b>0.150</b>	<b>0.290</b>	0.317	0.388	0.449	<b>0.3906</b>	<b>0.390</b>
		<b>0</b>	<b>0</b>	<b>0</b>	<b>3</b>	0	8	2		<b>6</b>
KANO STATE	Activation functions	Training: 70%; Testing: 30%			Training:80%; Testing:20%			Training:90%; Testing:10%		
		Hidden layer (1)	Hidden layer (2)	Hidden layer (3)	Hidden layer (1)	Hidden layer (2)	Hidden layer (3)	Hidden layer (1)	Hidden layer (2)	Hidden layer (3)
		n	n	n	n	n	n	n	n	n
	RELU	<b>0.861</b>	1.041	1.039	<b>1.103</b>	1.246	1.238	<b>1.648</b>	1.6496	1.755
		<b>8</b>	1	6	<b>5</b>	2	9	<b>0</b>		2
	Sigmoid	1.125	<b>0.822</b>	1.139	1.118	<b>1.073</b>	1.187	1.847	<b>1.6085</b>	1.745
		6	<b>6</b>	7	3	<b>1</b>	3	2		8
	Hyperbolic tangent	1.173	<b>1.129</b>	1.170	<b>1.106</b>	1.119	1.148	1.787	1.9466	<b>1.668</b>
		6	<b>7</b>	4	<b>8</b>	9	9	3		<b>6</b>
	KEBBI STATE	Activation functions	Training: 70%; Testing: 30%			Training:80%; Testing:20%			Training:90%; Testing:10%	
Hidden layer (1)			Hidden layer (2)	Hidden layer (3)	Hidden layer (1)	Hidden layer (2)	Hidden layer (3)	Hidden layer (1)	Hidden layer (2)	Hidden layer (3)
n			n	n	n	n	n	n	n	n
RELU		0.187	<b>0.162</b>	0.248	0.174	<b>0.167</b>	0.170	0.227	0.2275	<b>0.227</b>
		8	<b>6</b>	6	8	<b>9</b>	2	5	1	<b>4</b>
Sigmoid		<b>0.163</b>	0.230	0.176	0.203	<b>0.150</b>	1.302	<b>0.206</b>	0.2197	0.652
		<b>0</b>	7	4	9	<b>7</b>	3	<b>0</b>		5
Hyperbolic tangent		0.299	0.207	0.210	0.202	<b>0.155</b>	0.710	<b>0.263</b>	0.5351	0.717
		2	1	7	8	<b>8</b>	4	<b>8</b>		3
SOKOTO STATE		Activation functions	Training: 70%; Testing: 30%			Training:80%; Testing:20%			Training:90%; Testing:10%	
	Hidden layer (1)		Hidden layer (2)	Hidden layer (3)	Hidden layer (1)	Hidden layer (2)	Hidden layer (3)	Hidden layer (1)	Hidden layer (2)	Hidden layer (3)
	n		n	n	n	n	n	n	n	n
	RELU	0.716	1.191	<b>0.125</b>	<b>0.717</b>	0.975	0.963	1.182	1.1827	<b>1.175</b>
		2	0	<b>4</b>	<b>3</b>	8	6	6		<b>7</b>

	Sigmoid	<b>0.905</b>	1.149	0.929	1.125	<b>1.031</b>	1.162	1.813	1.1793	<b>1.336</b>
		<b>9</b>	1	0	9	<b>7</b>	4	4		<b>8</b>
	Hyperbol	1.271	<b>0.853</b>	1.437	0.723	<b>0.717</b>	1.390	2.443	<b>1.2458</b>	1.573
	ic tangent	4	<b>4</b>	2	0	<b>0</b>	1	6		6

---

ZAMFAR	Activatio	Training: 70%;			Training:80%;			Training:90%;		
		Testing: 30%			Testing:20%			Testing:10%		
A	n	Hide	Hide	Hide	Hide	Hide	Hide	Hide	Hide	Hide
STATE	functions	n	n	n	n	n	n	n	n layer	n
		layer	layer	layer	layer	layer	layer	layer	(2)	layer
		(1)	(2)	(3)	(1)	(2)	(3)	(1)		(3)
	RELU	0.262	0.104	<b>0.100</b>	0.368	0.148	<b>0.146</b>	0.071	0.0716	<b>0.071</b>
		0	0	<b>6</b>	0	4	<b>8</b>	6		<b>5</b>
	Sigmoid	0.170	0.281	<b>0.135</b>	0.367	<b>0.016</b>	0.032	0.007	0.0150	<b>0.005</b>
		4	8	<b>6</b>	8	<b>0</b>	0	4		<b>2</b>
	Hyperbol	0.065	<b>0.050</b>	0.061	0.186	0.359	<b>0.033</b>	0.012	<b>0.0082</b>	0.014
	ic tangent	5	<b>1</b>	5	4	5	<b>7</b>	3		4

The minimum mean square error (MSE) values in Katsina state are as follows: RELU (0.0993) has the lowest MSE value at the 70% training set, RELU (0.1251) at the 80% training set, and Sigmoid (1.6085) at the 90% training set. Consequently, with a 70% training set, RELU has the lowest MSE value. The least mean square error (MSE) in Kano state is found at 70% training set for Sigmoid (0.8226), 80% training set for Sigmoid (1.0731), and 90% training set for Sigmoid (1.6085). Consequently, at 70% of the training set, sigmoid has the lowest MSE value. In Kebbi state, the lowest MSE value is found at 70% training set for ReLU (0.1626), 80% training set for Sigmoid (0.1507), and 90% training set for Sigmoid (0.2060). Sigmoid, then, has the lowest MSE value at 80% of the training set. In the state of Sokoto, the minimal mean square error (MSE) is found for ReLU (0.1254) at 70% training set, Hyperbolic tangent (0.7170) at 80% training set, and Sigmoid (1.3368) at 90% training set. ReLU, thus, has the lowest MSE value at 70% of the training set. The minimal MSE values in Zamfara state are found at 70% training set for the hyperbolic tangent (0.0501), 80% training set for Sigmoid (0.0160), and 90% training set for Sigmoid (0.0052). Sigmoid has the lowest MSE value at 90% training set as a result. In conclusion, Sigmoid fared better in the North West than the other activation functions. In Kano, Kebbi, and Zamfara states, respectively, it has the lowest MSE.

#### 4. Conclusion

Researchers and professionals working on droughts have found that evaluating droughts is a difficult undertaking. In order to evaluate the impact of drought indicators on maize output in Northern Nigeria, artificial neural networks (ANNs) were used in this study to examine the performance of four drought indices: RDI, SCWLPM, SCPHDI, and SCPDSI. The majority of the lowest mean square errors (MSEs) across the states were generated by RELU while taking the activation function into consideration. When analyzing the effects of drought in Northern Nigeria, the Artificial Neural Network's RELU activation function works best. Moreover, the mean square error rises in tandem with the training percentage. In the North Central region, Plateau state has the lowest Mean Squared

Error (0.0346) for ANN. The state of Borno in the northeastern area has the lowest ANN MSE (0.0732). In the northwest area, Zamfara state had the lowest MSE for ANN (0.0052).

### Authors Contribution

Dr. Adedayo A. Adopaju supervised the work and also writing and editing. Grace A. Awomokun did the writing of the original draft and Tayo P. Ogundunmade worked on the methodology, writing and editing.

### References

- [1] Abaje, I.B., O.F. Ati, E.O. Iguisi, and G.G. Jidauna. (2013). Droughts in the Sudano-Sahelian Ecological Zone of Nigeria: Implications for Agriculture and Water Resources Development. *Global Journal of Human Social Science* 13 (2): 12–23.
- [2] Barua S, Ng AWM, Perera BJC. (2012). Artificial neural network-based drought forecasting using a non-linear aggregated drought index. *J Hydrol Eng*; 17(12): 1408- 1413.
- [3] Bates, B.C., Kundzewicz, Z.W., Wu, S. and Palutikof, J.P. (Eds). (2008). *Climate Change and Water*. Technical Paper of the Intergovernmental Panel on Climate Change, IPCC Secretariat, Geneva. Available from <https://www.ipcc.ch/pdf/technical-papers/climate-change-water-en.pdf> - 28/doc13.pdf (accessed: June, 2018).
- [4] Birikundavyi S, Labib R, Trung HT, Rousselle J. (2002). Performance of neural networks in daily streamflow forecasting. *J Hydrolog Eng*; 7(5): 392- 398.
- [5] Dai A. (2011). Drought under global warming: a review. *Wiley Interdisciplinary Reviews: Climate Change* 2 (1), 45–65.
- [6] Deo RC, Sahin M. (2015). Application of the artificial neural network model for prediction of monthly standardized precipitation and evapotranspiration index using hydrometeorological parameters and climate indices in eastern Australia. *Atmos Res*. 2015; 161(162): 65- 81. <https://doi.org/10.1016/j.atmosres.2015.03.018>.
- [7] Deo RC, Sahin M. (2015). Application of the artificial neural network model for prediction of monthly standardized precipitation and evapotranspiration index using hydrometeorological parameters and climate indices in eastern Australia. *Atmos Res*. 2015; 161(162): 65- 81. <https://doi.org/10.1016/j.atmosres.2015.03.018>.
- [8] Eze, J.N. (2017). Assessment of Household Vulnerability and Adaptation to Desertification in Yobe State, Nigeria, A thesis submitted to the School of Postgraduate studies and the Department of Geography. Nsukka in Partial Fulfillment of the Requirements for the Degree of Doctor of Philosophy: University of Nigeria.
- [9] Eze, J.N., U. Aliyu, A. Alhaji-Baba, and M. Alfa. (2018). Analysis of farmers' vulnerability to climate change in Niger state, Nigeria. *International Letters of Social and Humanistic Sciences*. 82: 1–9.
- [10] FAOSTAT. (2018). *Production Statistics (Prodstat)*; Food and Agriculture Organization of the United Nations: Rome, Italy.
- [11] Fung KF, Huang YF, Koo CH, Mirzaei M. (2019). Improved SVR machine learning models for agricultural drought prediction at downstream of Langat River Basin. *Malaysia J Water Climate Change*; 10(2): 1– 16. <https://doi.org/10.2166/wcc.2019.295>.
- [12] Ghumman AR, Ghazaw YM, Sohail AR, Watanabe K. (2011). Runoff forecasting by artificial neural network and conventional model. *Alex Eng J*; 50: 345- 350.
- [13] Gidey, E., O. Dikinya, R. Sebego, E. Segosebe, and A. Zenebe. (2018). Analysis of the long-term agricultural drought onset, cessation, duration, frequency, severity and spatial extent using vegetation health index (VHI) in Raya and its environs, northern Ethiopia. *Environmental Research System* 7 (13). <https://doi.org/10.1186/s40068-018-0115-z>.
- [14] Hai T, Sharafati A, Mohammed A, et al. (2020). Global solar radiation estimation and climatic variability analysis using extreme learning machine based predictive model. *IEEE Access*. 2020; 14(8): 12026– 12042. <https://doi.org/10.1109/ACCESS.2020.2965303>.
- [15] Kamara A.Y., Kamai N., Omoigui L.O., Togola A., and Onyibe J.E. (2020). *Guide to Maize Production in Northern Nigeria*: Ibadan, Nigeria. 18 pp.
- [16] Kamara, A.Y., S.U. Ewansiha, and A. Menkir. (2014). Assessment of nitrogen uptake and utilization in drought-tolerant and Striga resistant tropical maize varieties. *Archives of Agronomy and Soil Science* 60: 195–207. doi:10.1080/03650340.2013.783204
- [17] Leste, RB. (2006). *The earth is shrinking: Advancing deserts and rising seas squeezing civilization*. Earth Policy Institute.

- [18] Liu, Xianfeng, Xiufang ZHU, Yaozhong PAN, Jianjun BAI, and Shuangshuang LI. (2018). Performance of different drought indices for agriculture drought in the North China plain. *Journal of Arid Land*. <https://doi.org/10.1007/s40333-018-0005-2>.
- [19] Morid S, Smakhtin V, Bagherzadeh K. (2007). Drought forecasting using artificial neural networks and time series of drought indices. *Int J Climatol*; 27: 2103- 2111.
- [20] Nyong AF, Adesina, Elasha BO (2007). The Value of Indegenous Knowledge in Climate change Mitigation and Adaptation Strategies in the African Sahel. *Mitigation and Adaptation Strategies for Global Change* 12: 787-797.
- [21] Shiru, M.S., S. Shahid, N. Alias, and E.S. Chung. (2018). Trend analysis of droughts during crop growing seasons of Nigeria. *Sustainability* 10 (871): 1–13. <https://doi.org/10.3390/su10030871>.
- [22] Tihamiyu, S.A., J.N. Eze, T.M. Yusuf, A.T. Maji, and S.O. Bakare. (2015). Rainfall variability and its effect on yield of Rice in Nigeria. *International Letters of Natural Sciences* 49: 63–68.
- [23] Tsakiris, G., and Vangelis, H. (2005). “Establishing a drought index incorporating evapotranspiration”. *European Water*, 9 (10): 3–11.
- [24] Um, M., Y. Kim, D. Park, and J. Kim. (2017). Effects of different reference periods on drought index estimations from 1901 to 2014. *Hydrology and Earth System Sciences* 21: 4989–5007.
- [25] Wang W, Van Gelder P, Vrijling JK, Ma J. (2006). Forecasting daily streamflow using hybrid ANN models. *J Hydrol*; 324: 383- 399.
- [26] Yue, Y., S. Shen, and Q. Wang. (2018). Trend and variability in droughts in Northeast China based on the reconnaissance drought index. *Water* 10 (318): 1–17.
- [27] Faiz, M. A., Zhang, Y., Ma, N., Baig, F., Naz, F., & Niaz, Y. (2021). Drought indices: aggregation is necessary or is it only the researcher’s choice? *Water Supply*, 00(0), 1–16. <https://doi.org/10.2166/ws.2021.163>
- [28] Sarki, Ahmed & Roni, Babangida. (2019). This disease is “not for hospital”: myths and misconceptions about cancers in Northern Nigeria. *Journal of Global Health Reports*. 3. [10.29392/joghr.3.e2019070](https://doi.org/10.29392/joghr.3.e2019070).